Article

Cell

Single-Cell Genomics Unveils Critical Regulators of Th17 Cell Pathogenicity

Graphical Abstract

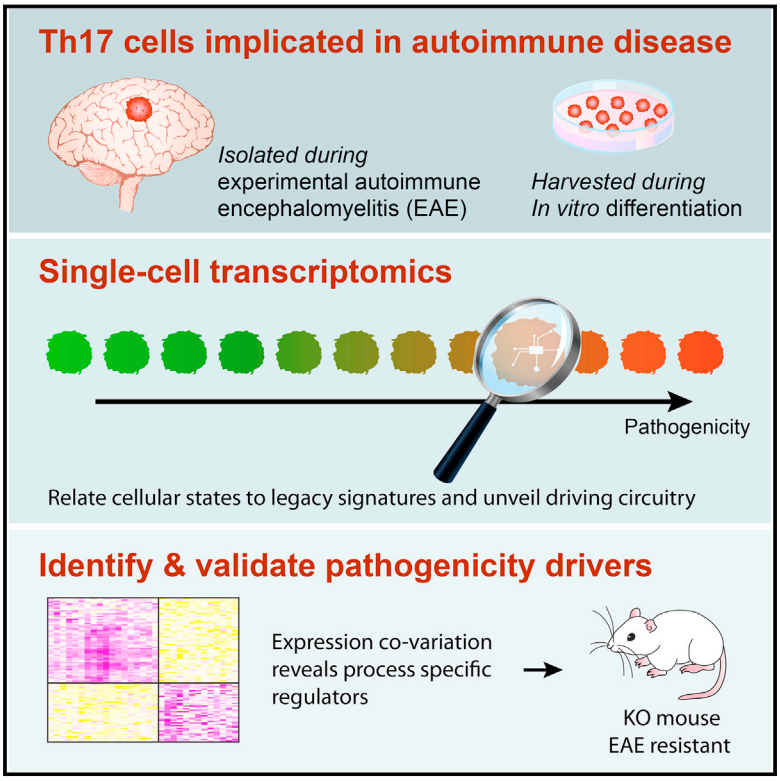

Authors

Jellert T. Gaublomme, Nir Yosef, Youjin Lee, ..., Vijay K. Kuchroo, Hongkun Park, Aviv Regev

Correspondence

hongkun_park@harvard.edu (H.P.), aregev@broadinstitute.org (A.R.)

In Brief

Single-cell RNA-seq coupled to a new functional annotation approach identifies distinct functional states of Th17 cells and the underlying molecular mechanisms that regulate their pathogenicity.

Highlights

- Atlas of Th17 single-cell RNA-seq profiles reveals extensive heterogeneity
- Annotation approach relates single-cell profiles to legacy genomic signatures
- Pathogenicity regulators co-vary with pro-inflammatory and regulatory modules
- Functional validation of Th17 pathogenicity regulators: GRP65, TOSO, and PLZP

Accession Numbers

GSE74833

Gaublomme et al., 2015, Cell *163*, 1–13
December 3, 2015 ©2015 Elsevier Inc.
http://dx.doi.org/10.1016/j.cell.2015.11.009

CellPress

Please cite this article in press as: Gaublomme et al., Single-Cell Genomics Unveils Critical Regulators of Th17 Cell Pathogenicity, Cell (2015), http://dx.doi.org/10.1016/j.cell.2015.11.009

Article

Cell

Single-Cell Genomics Unveils Critical Regulators of Th17 Cell Pathogenicity

Jellert T. Gaublomme,[1,2,3,14] Nir Yosef,[1,4,14] Youjin Lee,[1,5,14] Rona S. Gertner,[2,3] Li V. Yang,[6] Chuan Wu,[5] Pier Paolo Pandolfi,[7] Tak Mak,[8] Rahul Satija,[1,9,10] Alex K. Shalek,[1,11,12] Vijay K. Kuchroo,[1,5,15] Hongkun Park,[1,2,3,15,*] and Aviv Regev[1,13,15,*]

[1]Broad Institute of MIT and Harvard, 415 Main Street, Cambridge, MA 02142, USA
[2]Department of Chemistry and Chemical Biology, Harvard University, 12 Oxford Street, Cambridge, MA 02138, USA
[3]Department of Physics, Harvard University, 17 Oxford Street, Cambridge, MA 02138, USA
[4]Department of Electrical Engineering and Computer Science and Center for Computational Biology, University of California, Berkeley, Berkeley, CA 94720, USA
[5]Evergrande Center for Immunologic Diseases, Harvard Medical School and Brigham and Women's Hospital, Harvard Institutes of Medicine, 77 Avenue Louis Pasteur, Boston, MA 02115, USA
[6]Department of Internal Medicine, Department of Anatomy and Cell Biology, Brody School of Medicine, East Carolina University, Greenville, NC 27834, USA
[7]Cancer Research Institute, Beth Israel Deaconess Cancer Center, Department of Medicine and Pathology, Beth Israel Deaconess Medical Center, Harvard Medical School, Boston, MA 02215, USA
[8]Ontario Cancer Center, Princess Margaret Hospital, Toronto, ON M5G 2M9, Canada
[9]New York Genome Center, New York, NY 10013, USA
[10]Center for Genomics and Systems Biology, New York University, New York, NY 10012, USA
[11]Institute for Medical Engineering and Science and Department of Chemistry, Massachusetts Institute of Technology, Cambridge, MA 02142, USA
[12]Ragon Institute of Massachusetts General Hospital, Massachusetts Institute of Technology and Harvard University, Boston, MA 02139, USA
[13]Howard Hughes Medical Institute and David H. Koch Institute of Integrative Cancer Biology, Department of Biology, Massachusetts Institute of Technology, Cambridge, MA 02142, USA
[14]Co-first author
[15]Co-senior author
*Correspondence: hongkun_park@harvard.edu (H.P.), aregev@broadinstitute.org (A.R.)
http://dx.doi.org/10.1016/j.cell.2015.11.009

SUMMARY

Extensive cellular heterogeneity exists within specific immune-cell subtypes classified as a single lineage, but its molecular underpinnings are rarely characterized at a genomic scale. Here, we use single-cell RNA-seq to investigate the molecular mechanisms governing heterogeneity and pathogenicity of Th17 cells isolated from the central nervous system (CNS) and lymph nodes (LN) at the peak of autoimmune encephalomyelitis (EAE) or differentiated in vitro under either pathogenic or non-pathogenic polarization conditions. Computational analysis relates a spectrum of cellular states in vivo to in-vitro-differentiated Th17 cells and unveils genes governing pathogenicity and disease susceptibility. Using knockout mice, we validate four new genes: *Gpr65*, *Plzp*, *Toso*, and *Cd5l* (in a companion paper). Cellular heterogeneity thus informs Th17 function in autoimmunity and can identify targets for selective suppression of pathogenic Th17 cells while potentially sparing non-pathogenic tissue-protective ones.

INTRODUCTION

The immune system strikes a balance between mounting proper responses to pathogens and avoiding autoimmune reactions. In particular, as part of the adaptive immune system, pro-inflammatory IL-17-producing Th17 cells mediate clearance of fungal infections and other pathogens (Hernández-Santos and Gaffen, 2012) and maintain mucosal barrier functions (Blaschitz and Raffatellu, 2010) but are also implicated in pathogenesis of autoimmunity (Korn et al., 2009).

Mirroring this functional diversity, in vitro polarized Th17 cells can either cause severe autoimmune responses upon adoptive transfer ("pathogenic," polarized with IL-1β+IL-6+IL-23) or have little or no effect in inducing autoimmune disease ("non-pathogenic," polarized with TGF-β1+IL-6) (Ghoreschi et al., 2010; Lee et al., 2012).

Analysis of these states has been limited, however, by relying either on genomic profiling of cell populations, which cannot distinguish distinct states within them, or on tracking a few known markers by flow cytometry (Perfetto et al., 2004). Single-cell RNA-seq (Shalek et al., 2013, 2014; Trapnell et al., 2014) opens the way for a more unbiased interrogation of cell states, including in limited in vivo samples.

Please cite this article in press as: Gaublomme et al., Single-Cell Genomics Unveils Critical Regulators of Th17 Cell Pathogenicity, Cell (2015), http://dx.doi.org/10.1016/j.cell.2015.11.009

Here, we use single-cell RNA-seq to show that cells isolated from the draining LNs and CNS at the peak of EAE exhibit diverse functional states, and we relate them to a spectrum spanning from more regulatory to more pathogenic cells observed in Th17 cells polarized in vitro. Genes associated with these opposing states include both canonical known regulators and novel candidates. We validated four high-ranking candidates—*Gpr65*, *Plzp*, *Toso*, and *Cd5l* (the latter in a companion study in this issue of *Cell* [Wang et al., 2015])—with knockout mice, uncovering substantial effects on in vitro differentiation and in vivo EAE development.

RESULTS

RNA-Seq Profiling of Single Th17 Cells Isolated In Vivo and In Vitro

We profiled the transcriptome of 976 Th17 cells (ultimately retaining 722 cells, below), either harvested in vivo or differentiated in vitro (Figure 1A, Table S1, and Experimental Procedures). In vivo, we induced EAE by myelin oligodendrocyte glycoprotein (MOG_{35-55}) immunization, harvested $CD3^+CD4^+$IL-17A/GFP^+ cells from the draining LNs and CNS at the peak of disease, and profiled them promptly. In vitro, we profiled $CD4^+$ naive T cells at 48 hr of activation under TGF-β1+IL-6 or IL-1β+IL-6+IL-23. We prepared mRNA SMART-seq libraries using microfluidic chips (Fluidigm C_1), followed by transposon-based library construction.

We removed 254 cells (~26%) by quality metrics (Supplemental Experimental Procedures), and we controlled for quantitative confounders and batch effects (Experimental Procedures and Figures S1A and S1B). We retained ~7,000 appreciably expressed genes (fragments per kilobase of exon per million [FPKM] > 10 in at least 20% of cells in each sample) for in vitro experiments and ~4,000 for in vivo ones. To account for expressed transcripts that are not detected (false negatives) due to the limitations of single-cell RNA-seq (Deng et al., 2014; Shalek et al., 2014), we down-weighted the contribution of less reliably measured transcripts (Figure S1C and Experimental Procedures). Following these filters, expression profiles tightly correlated between population replicates (Figure 1B) and between the average expression across single cells and the matching population profile ($r \sim 0.65$–0.93; Figures 1C, S1D, and S2). However, we found substantial differences in expression between individual cells in the same condition ($r \sim 0.45$–0.75, Figures 1D, 1E, and S1D), comparable to previous observations in other immune cells (Shalek et al., 2014). We validated the observed expression patterns for eight representative genes with flow RNA-fluorescence in situ hybridization (Supplemental Experimental Procedures) (Figures 1F, 1G, and S1E). While most transcripts (e.g., *Irf4*, *Batf*, *Actb*) are expressed unimodally or nearly so (e.g., *Rorc*), some key transcripts (e.g., *Il17a*) exhibit a bimodal distribution, suggesting functional variation.

A Functional Annotation of Single-Cell Heterogeneity Shows that Th17 Cells Span a Spectrum of States In Vivo

To study the main sources of cellular variation in vivo, we used a principal component analysis (PCA, Figure 2A) followed by a novel analysis for functional annotation of the principal component (PC) space based on the single-cell expression of gene signatures of known T cell states (Figure 2B and Experimental Procedures), such that each signature is scored for its association with each PC. To identify transcription factors that may orchestrate this heterogeneity, we identified factors whose targets are strongly enriched (Fisher's exact test, $p < 10^{-5}$) in genes that correlated with each PC (Pearson correlation, FDR < 0.05; Figures 2E and 2F and Table S3).

The first PC (PC1) positively correlates with a recently defined effector versus memory signature following viral infection (Crawford et al., 2014) and negatively correlates with a signature characterizing memory T cells (Wherry et al., 2007) (Figure 2A and Table S2). This suggests that cells span from effector (high positive PC1 scores) to memory (high negative PC1 scores) phenotypes. PC2 separates cells by their source of origin (CNS or LN) and correlates with a transition from a naive-like state (negatively correlated with PC2; $p < 10^{-42}$, Figure 2A and Table S2) with low cell-cycle activity (FDR < 5%) to a Th1-like effector or memory effector state (positively correlated with PC2, Figure 2A, $p < 10^{-21}$ and $p < 10^{-57}$, respectively).

A Trajectory of Progressing Cell States from the LN to the CNS

To further explore the diversity of LN and CNS cells, we used five of the key signatures discovered by our functional annotation to define Voronoi regions that divide the PCA space into subpopulations of cells (Supplemental Experimental Procedures, Figure 2C, and Table S2). We identified genes characterizing each group by differential expression (KS test, FDR < 0.05; Table S4). For brevity, we assign new labels to these subpopulations (Th17 self-renewing, Th17/Th1-like effector, etc.), based on strong correlation with previous signatures and known genes (below); any such label may inevitably fall short of capturing the complex underlying biology.

Overall, the cells gradually progress through from a self-renewing-like state in the LN to a pre-Th1 effector-like phenotype in the LN and CNS to a Th1-like effector state and a Th1-like memory state in the CNS and, finally, a less functional state in the CNS. First, self-renewing-like Th17 cells in the LN (Figure 2C) are characterized by: (1) a signature of Wnt signaling ($p < 10^{-4}$, KS test comparing the signature score to all other subpopulations; Figure 2A) (Reya et al., 2003) and high expression of *Tcf7* (Figure 2D), a key Wnt target and transcription factor regulating the stem cell-like state of Th17 cells (Muranski et al., 2011); (2) high expression of *Cd62l* (Figure 2D), a known naive state marker (De Rosa et al., 2001); and (3) upregulation (Figure 2D) of *Cd27*, a pro-survival gene lacking in short-lived T cells (Dolfi et al., 2008; Hendriks et al., 2000). Our analysis (Figure 2E) suggests that *Etv6*, *Med12*, and *Zfx* drive this self-renewing population (Discussion). Next, cells from the LN and CNS adopt similar (overlapping) cell states in the central region of our PCA plot (Figure 2C), reflecting effector Th17-like cells with a pre-Th1-like phenotype, characterized by induction of receptors for IFN (*Ifngr2*) and IL-18 (*Il18r1*, Figure 2D) (Holzer et al., 2013), and of chemokine receptors *Cxcr6* (Figure 2D) (Aust et al., 2005) and *Ccr2* (Figure 2D) (Mahad and Ransohoff, 2003), which may all poise the cells for recruitment to the CNS. In turn, IL-17A/GFP^+-sorted cells acquire a Th17/Th1-like effector phenotype in the CNS (Figure 2C),

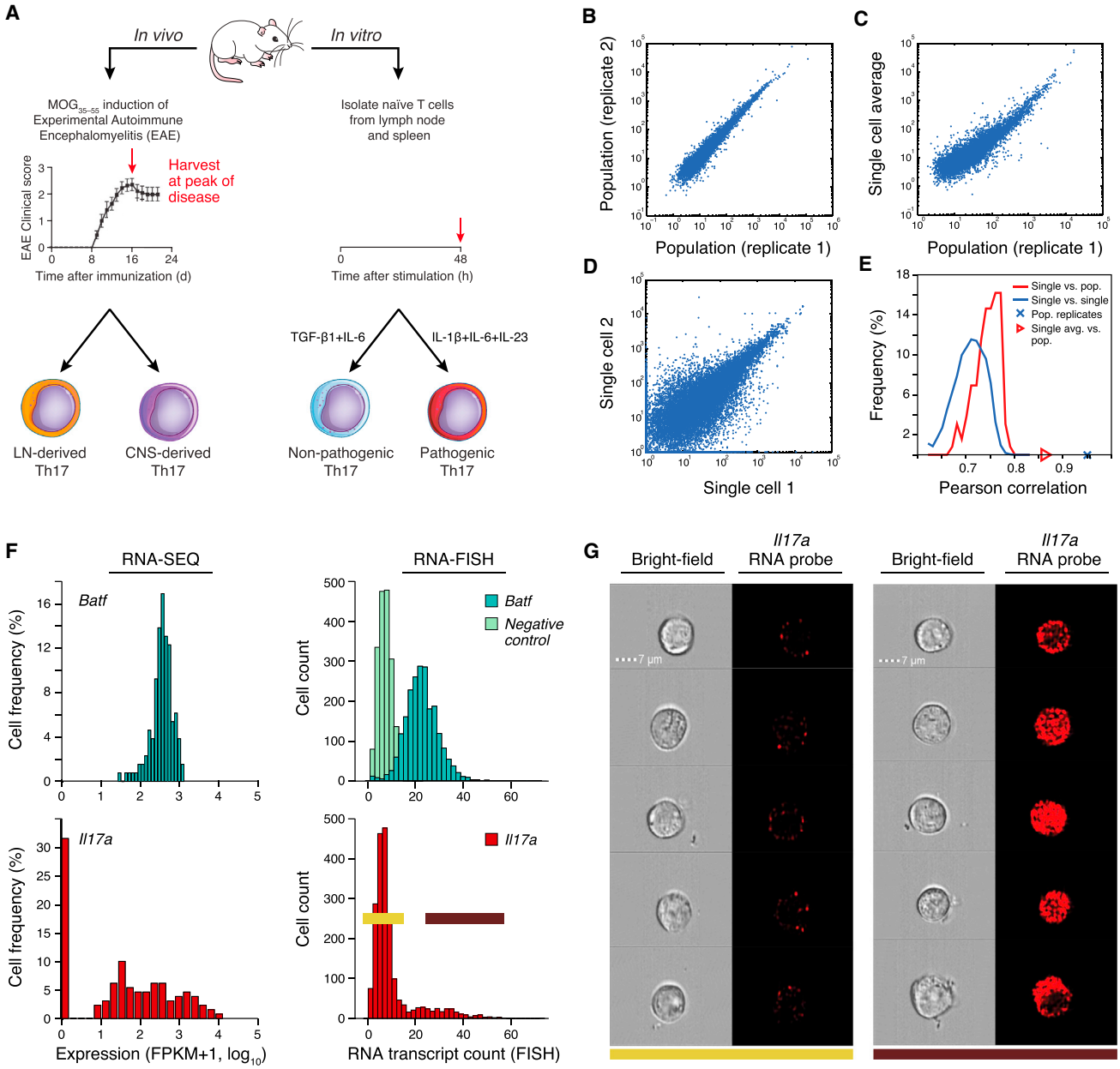

Figure 1. Single-Cell RNA-Seq of Th17 Cells In Vivo and In Vitro

(A) Experimental setup.

(B–E) Quality of single-cell RNA-seq. Scatter plots (B–D) compare transcript expression (FPKM+1, $\log_{10}$) from the in vitro TGF-β1+IL-6 48 hr condition between two bulk population replicates (B), the "average" of single-cell profile and a matched bulk population control (C), or two single cells (D). Histograms (E) depict the distributions of Pearson correlation coefficients (x axis) between single cells and their matched population control and between pairs of single cells.

(F and G) Comparison to RNA Flow-FISH. (F) Expression distributions by RNA-seq and RNA Flow-FISH at 48 hr under the TGF-β1+IL-6 in vitro condition. Negative control: bacterial *DapB* gene.

(G) Bright-field and fluorescence channel images of RNA Flow-FISH in negative (left) and positive (right) cells.

See also Figure S1 and Table S1.

with upregulation ($p < 10^{-3}$, KS test, Table S4) of: *Ifn-γ* (Figure 2D), *Rankl,* (*Tnfsf11*) (Nakae et al., 2007; Komatsu et al., 2014), and cell-cycle genes (e.g., *Geminin,* Figure 2D), a strong correlation with a salt-induced pathogenic Th17 cell signature (Wu et al., 2013) (Figure 2A), and association with both canonical Th17 TFs (*Stat3* and *Hif1a*) and Th1-associated factors, including *Rel* and *Stat4* (Figure 2E), which are associated with EAE (Hilliard et al., 2002; Mo et al., 2008) or with human autoimmune disease (Gilmore and Gerondakis, 2011). These cells could either be stable "double producers" or could reflect Th17 plasticity into the

Please cite this article in press as: Gaublomme et al., Single-Cell Genomics Unveils Critical Regulators of Th17 Cell Pathogenicity, Cell (2015), http://dx.doi.org/10.1016/j.cell.2015.11.009

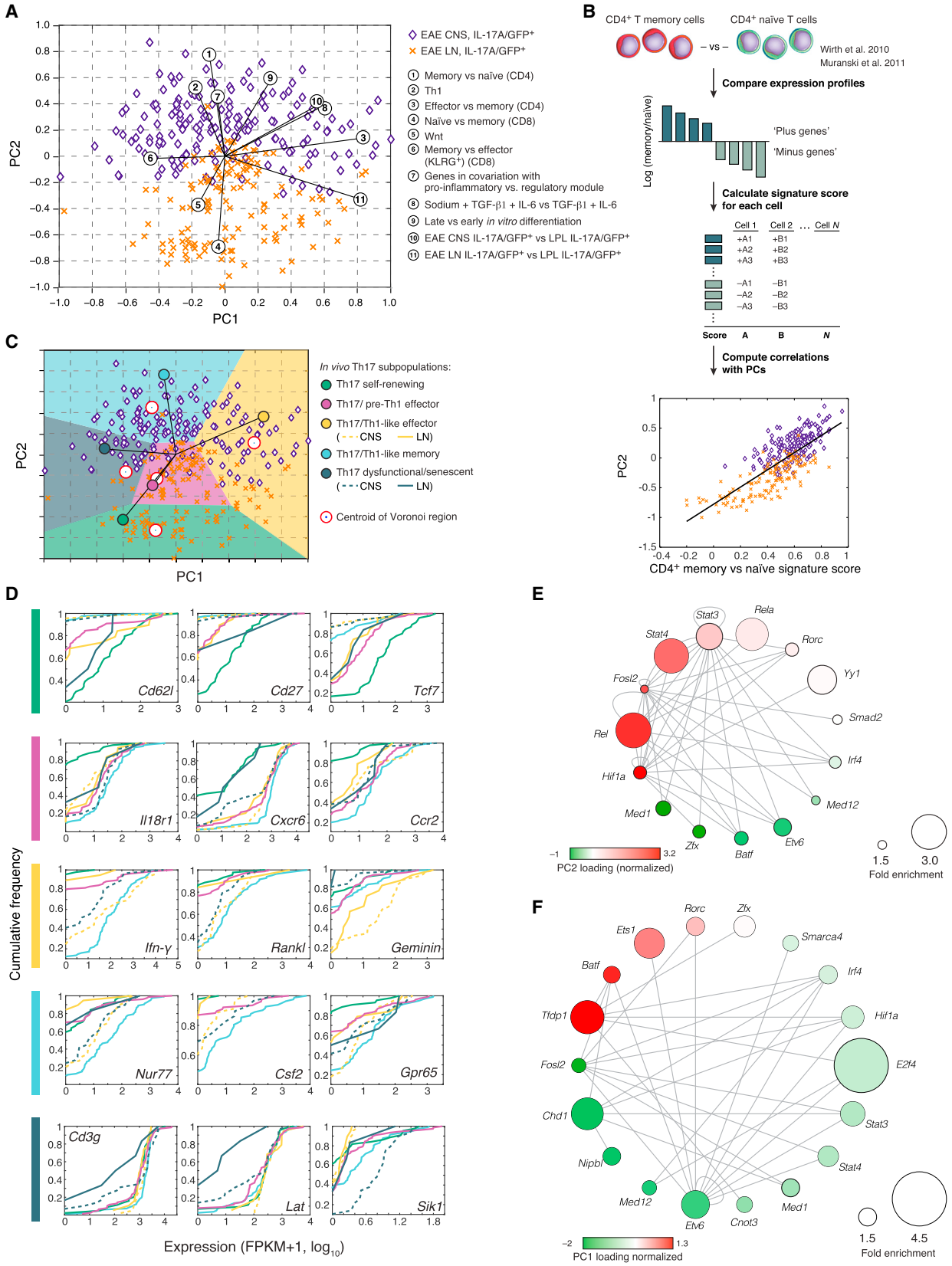

(legend on next page)

Th1 lineage (Discussion). Next, Th1-like memory cells detected in the CNS (Figure 2C) correlate highly with both a memory phenotype (negative PC1) and a Th1-like phenotype (positive PC2), upregulating ($p < 10^{-3}$, KS test, Table S4) memory signature genes (e.g., *Nur77*, *Samsn1*, *Il2ra*, *Il2rb*, *Tigit*, *Ifngr1*, and *Il1r2*) and pro-inflammatory genes (*Csf2* and *Gpr65*; Figure 2D) and associated with *Hif1a* regulation (Figure 2F), crucial for controlling human Th17 cells to become long-lived effector memory cells (Kryczek et al., 2011). Finally, a few Th17 cells may even acquire a somewhat senescent-like phenotype in the CNS (negative PC1 and PC2 scores; Figure 2C), correlating with a signature comparing CD4 T cells at day 30 during a chronic infection to those during acute infection (Table S2) and downregulation ($p \sim 10^{-2}$, KS test, Table S4) of some T cell activation genes (Figure 2D and Table S4).

Further supporting the interpretation of gradual progression, most in vivo cells are maximally correlated with bulk profiles at 48–72 hr during Th17 cell differentiation in vitro (Yosef et al., 2013) (Figure S4B), but some cells, especially from the LN, correlate most strongly with earlier time points. Indeed, time point annotations positively correlate with PC2 ($r \sim 0.5$; $p < 10^{-27}$, Figures 2A and S4D). Finally, a population-based signature comparing profiles of EAE Th17 cells to lamina propria lymphocyte (LPL) Th17 cells (Supplemental Experimental Procedures and Figure S3), which are known to assume a regulatory phenotype (Esplugues et al., 2011; O'Connor et al., 2009), correlates with PC1 in vivo ($p < 10^{-25}$, Figure 2A, Table S2), indicating that EAE-derived Th17 cells adopt a stronger effector phenotype than gut-derived Th17 cells.

In-Vitro-Derived Cells Span a Spectrum of Pathogenicity States with Similarities and Distinctions from In Vivo Isolated Cells

Given the limited cell availability from in vivo samples and the fact that cells are obtained as a mixed "snapshot" of an asynchronous process, it is difficult to further characterize their distinct pathogenic potential. A complementary strategy is to profile Th17 cells differentiated in vitro and compare in vivo and in vitro profiles.

We analyzed single-cell RNA-seq profiles of 420 Th17 cells derived under non-pathogenic (TGF-β1+IL-6, unsorted: 130 cells from 2 biological replicates and TGF-β1+IL-6; sorted for IL-17A/GFP$^+$: 151 cells from 3 biological replicates) and pathogenic conditions (Il-1β+IL-6+IL-23, sorted for IL-17A/GFP$^+$: 139 cells from 2 biological replicates) (Figure 3A).

Using our functional annotation approach (Figure 2B), we find that in-vitro-differentiated Th17 cells vary strongly in a key pathogenicity signature (Lee et al., 2012), reflecting their respective conditions (Figures 3A and 3D). High pathogenicity scores were associated with IL-17A/GFP$^+$-sorted cells polarized under the pathogenic condition (Figures 3A and 3D), whereas IL-17A/GFP$^+$-sorted cells from non-pathogenic conditions correlate highly with expression of regulatory cytokines (e.g., IL-10) and their targets, which are barely detected in pathogenic cells (Figure 3E). There is a zone of overlap in cell states between the pathogenic and non-pathogenic conditions (Figure 3A), with cells polarized under the non-pathogenic (TGF-β1+IL-6) condition that were not sorted to be IL-17A/GFP$^+$ spanning the broadest pathogenicity spectrum (Figures 3A and 3D). A signature from *IL-23R*$^{-/-}$cells differentiated with IL-1β+IL-6+IL-23 (Y.L. and V.K.K, unpublished data) correlates highly with the more regulatory cells, confirming the role of the IL-23 pathway in pathogenicity (Figure 3A).

As expected, the most cells' profiles correlate with bulk profiles at 48–50 hr (Yosef et al., 2013) (Figure S4A). The correlated time points match with variation along PC2 (Figure 3A), but not PC1, suggesting that pathogenicity is not a reflection of the cell's position along the differentiation trajectory but is an orthogonal aspect of cell state.

To relate the in-vitro-differentiated cells to their in vivo counterparts, we scored the in vitro cells for signatures of immune-related genes that characterize the in-vivo-identified subpopulations (Figures 2C, 3B, and 3C and Supplemental Experimental Procedures). Cells derived in the non-pathogenic conditions score higher for the Th17 self-renewing-like signature ($p < 10^{-10}$, KS test; Table S2 and Figures 3A and 3C), whereas those derived in pathogenic conditions resemble the Th17/Th-1 like memory phenotype identified in the CNS ($p < 10^{-3}$, KS test; Figures 3A and 3B and Table S2).

Co-variation with Pro-inflammatory and Regulatory Modules in Th17 Cells Highlights Novel Candidate Regulators

We analyzed each gene's variation in expression across the unsorted cells from the TGF-β1+IL-6 differentiation condition. About 35% (2,252) of the detected genes are expressed

Figure 2. Th17 Cells Span a Progressive Trajectory of States from the LN to the CNS

(A) PCA separates CNS-derived cells from LN-derived cells. Shown are 302 cells in the space of the first two PCs. Numbered circles: signatures that significantly correlate with PC1 or PC2 ($p < 10^{-6}$, Table S2, Supplemental Experimental Procedures).

(B) Functional annotation. Top to bottom: Gene signatures are defined from literature, and a signature score is calculated for each single cell. The Pearson correlation coefficient is calculated between the signature score and the PC loading for each cell and PC and is plotted on the PCA plot (circled numbers in A) (Supplemental Experimental Procedures).

(C) Five progressive Th17 cell states from the LN to the CNS. Plot as in (A), but with Voronoi cells, defined by signatures (colored circles, Table S2) characterizing the cells populating the extremities of PCA space; five signature-specific subpopulations are marked. The self-renewing state was observed in two technical replicates of one of the two in vivo biological replicates, potentially due to differences in disease induction or progression.

(D) Example genes that distinguish each subpopulation. Cumulative distribution function (CDF) plots of expression for key selected genes. Dotted/solid line corresponds to CNS/LN cells, respectively, where appropriate.

(E and F) Transcription factors (nodes) whose targets are significantly enriched in PC2 (E) or PC1 (F). Nodes are sized proportionally to fold enrichment (Table S3) and are colored according to the loading of the encoding gene in the respective PC (loadings were normalized to have zero mean and SD of 1).

See also Figures S2, S3, and S4 and Tables S2, S3, and S4.

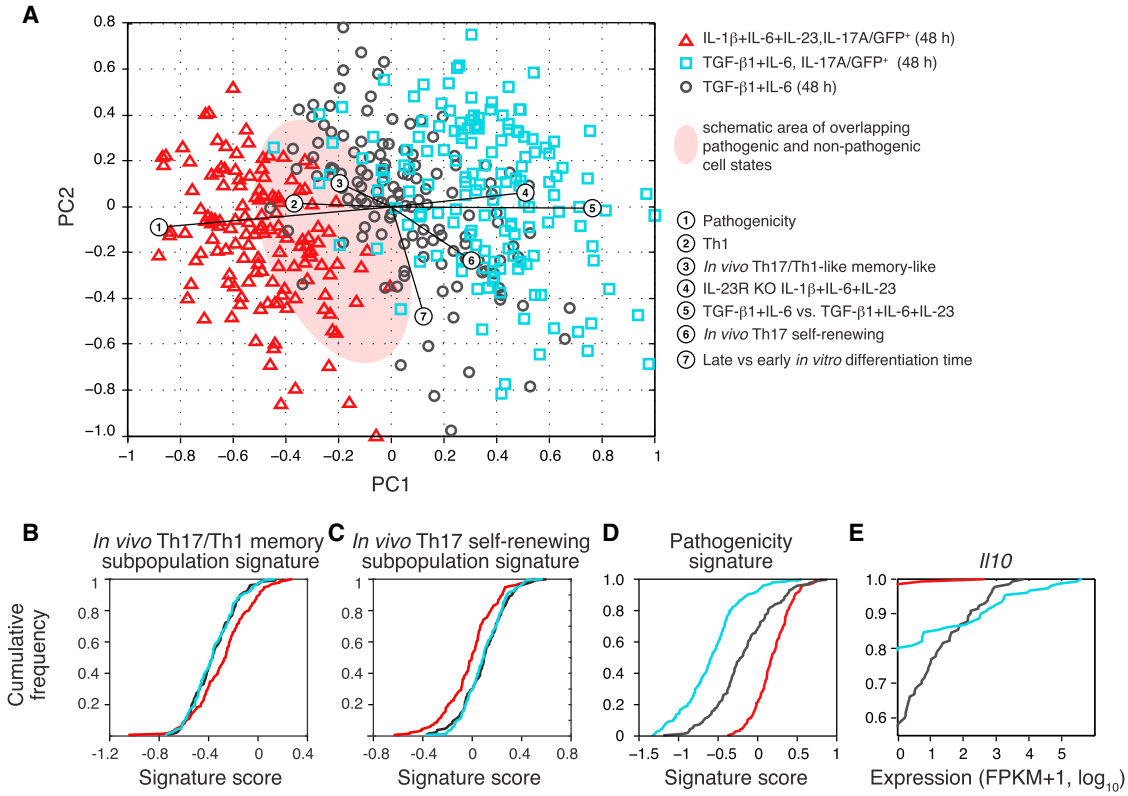

Figure 3. A Spectrum of Pathogenicity States In Vitro

(A) PCA plot of Th17 cells differentiated in vitro. PC1 separates cells from most (left) to least (right) pathogenic, as indicated by both the differentiation condition (color code) and the correlated signatures (numbered circles).

(B–D) Key signatures related to pathogenicity. CDFs of the single-cell scores for key signatures for the three in vitro populations (colored as in A): (B) a signature distinguishing the in vivo Th17/Th1-like memory subpopulation (blue in Figure 2C); (C) a signature distinguishing the in vivo Th17 self-renewing subpopulation (green in Figure 2C); and (D) a signature of pathogenic Th17 cells (Lee et al., 2012).

(E) CDFs of expression level (FPKM+1, $\log_{10}$) of *Il10* for the three in vitro populations.

See also Table S2.

in >90% of the cells (Figure 4A) with a unimodal distribution: these include housekeeping genes ($p < 10^{-10}$, hypergeometric test, Figures S5A and S5B), the Th17 signature cytokine *Il17f*, and transcription factors that are essential for Th17 differentiation (e.g., *Batf*, *Stat3*, *Rorc*, and *Hif1a*). Bimodally expressed genes—with high expression in at least 20% of the cells and much lower (often undetectable) levels in the rest—include inflammatory and regulatory cytokines and their receptors (e.g., *Il17a*, *Il10*, *Il21*, *Ccl20*, *Il24*, and *Il27ra*; Figure 4A). Expression variation may be more strongly related to pathogenicity than differentiation. Most (>75%) cells express pioneer and master transcription factors for the Th17 lineage (*Rorc*, *Irf4*, and *Batf*), but some also express transcripts encoding key genes from other T cell lineages (e.g., *Stat4* for Th1 cells, *Ccr4* for Th2 cells), suggesting the presence of previously reported "hybrid" double-positive cells (Antebi et al., 2013) and/or reflecting our model of duality in the Th17 transcriptional network (Yosef et al., 2013). The expression of many key immune genes varies more than that of other transcripts with the same mean expression level (Figure S5C), even when only considering the expressing cells (Figure S5D), implying a greater degree of diversity in immune-gene regulation. Such patterns must be interpreted with caution because some (e.g., *Il17a*, *Il24*, and *Ccl20*), but not all (e.g., *Il9*), of the transcripts with bi-modal patterns are lowly expressed and thus may be less reliably detected and also because transcription bursts coupled with transcript instability may lead to "random" fluctuations.

To overcome these challenges, we analyzed co-variation between transcripts across cells (Figure 4B), reasoning that, if variation reflects distinct cell states, entire gene modules should robustly co-vary across cells. Focusing on significant co-variation (Spearman correlation; FDR < 0.05) between bimodally expressed transcripts (expressed by less than 90% of cells; Figure 4B, rows, Supplemental Experimental Procedures) and a curated set of bimodally expressed immune response genes (Figure 4B, columns), we find two key transcript modules: one that co-varies with known pro-inflammatory Th17 cytokines, such as *Il17a* and *Ccl20*, and another that co-varies with known regulatory genes such as *Il10*, *Il24*, and *Il9*.

Using these modules as signatures to annotate the original in vitro cell states (Figure 4C), we find that a signature comparing the module co-varying with pro-inflammatory genes to the

module co-varying with regulatory genes strongly correlates with the most pathogenic cells (Figures 4C and 4D). We find further support from additional signatures and analyses: (1) a negative correlation between PC1 scores and a curated pathogenicity signature (Lee et al., 2012) and a positive correlation between PC1 and Tr1exTh17 cells versus Th17 cell signature (Gagliani et al., 2015) (Figure 4C and Table S2); (2) correlation with the inflammatory CNS-derived Th17 cells in vivo (Figure 2A); (3) enrichment of genes in the co-variation modules (rows of Figure 4B) for immune response genes (using MSigDB [Liberzon et al., 2011]; Table S5) for genes generically associated with inflammatory bowel disease (Jostins et al., 2012) and rheumatoid arthritis (Okada et al., 2014) ($p < 10^{-6}$; hypergeometric test) and for genes upregulated in cortical lesions derived from patients with progressive multiple sclerosis (Fischer et al., 2013) ($p < 0.02$, hypergeometric test).

These co-variation modules highlight novel putative regulators, many not detected or prioritized by previous population-level approaches (Ciofani et al., 2012; Yosef et al., 2013). We prioritized follow-up candidates with a computational ranking scheme (Experimental Procedures). While the genes from our co-variation matrix (rows, Figure 4B) tend to be highly ranked compared to all genes also in bulk-population data ($p < 10^{-10}$, Wilcoxon rank-sum test) or rankings (Ciofani et al., 2012) (Table S7 and Supplemental Experimental Procedures), they do not necessarily stand out in bulk population rankings (Figure S6), highlighting the distinct signal from single-cell profiles. Based on our ranking and knockout mice availability, we chose four genes novel to Th17 function for functional follow up: *Gpr65*, *Toso*, *Plzp*, and *Cd5l* (the latter presented in Wang et al., 2015).

Gpr65 Promotes Th17 Cell Pathogenicity and Is Essential for EAE

Gpr65, a glycosphingolipid receptor, is a member of the module co-varying with pro-inflammatory genes (Figure 4B) and is highly expressed in our Th1-like effector/memory cells (Figure 2D). Genetic variants in the *Gpr65* locus are associated with multiple sclerosis (Sawcer et al., 2011), ankylosing spondylitis (Cortes et al., 2013), inflammatory bowel disease (Jostins et al., 2012), and Crohn's disease (Franke et al., 2010).

Naive *Gpr65*$^{-/-}$ T cells differentiated with TGF-β1+IL-6 or IL-1β+IL-6+IL-23 for 96 hr show a ~40% reduction of IL-17A+ cells compared to WT controls (Figure 5A), as measured by intracellular cytokine staining (ICC, Supplemental Experimental Procedures). Memory cells from *Gpr65*$^{-/-}$ mice also showed an ~45% reduction in IL-17A+ cells after reactivation with IL-23 (Figure S7A). There was a reduced secretion of IL-17A ($p < 0.01$) and IL-17F ($p < 10^{-4}$) under pathogenic differentiation conditions in the knockout cells (Figure 5B) and increased IL-10 secretion ($p < 0.01$, Figure S7C) (Supplemental Experimental Procedures).

RNA-seq profiles (Supplemental Experimental Procedures) of populations of *Gpr65*$^{-/-}$ Th17 cells, differentiated under both non-pathogenic and pathogenic conditions for 96 hr, show that genes upregulated in *Gpr65*$^{-/-}$ cells are most strongly enriched ($p < 10^{-28}$, hypergeometric test, Figure 5E) for the genes characterizing the more regulatory Th17 cells (positive PC1, Figure 4C, Table S6, and Supplemental Experimental Procedures). Moreover, ChIP-seq analysis (Ciofani et al., 2012) indicates that *Rorγt*, the Th17 cell master transcription factor, binds the promoter region of *Gpr65*.

To determine the effect of loss of GPR65 on autoimmune disease, we reconstituted *RAG-1*$^{-/-}$ mice with naive WT or *Gpr65*$^{-/-}$ CD4$^+$ T cells and induced EAE (Supplemental Experimental Procedures). In the absence of *Gpr65*-expressing T cells, mice are protected from EAE (Figures 5D and S7D), and far fewer IL-17A and IFN-γ positive cells are recovered from the LN and spleen compared to WT controls (Figure S7B). Furthermore, in vitro restimulation with MOG_{35-55} of the spleen and LN cells from immunized mice showed that loss of GPR65 resulted in dramatic reduction of MOG_{35-55}-specific IL-17A or IFN-γ-positive cells (Figure 5C), suggesting that GPR65 regulates encephalitogenic T cells generation in vivo.

Toso Is Implicated in Th17 Pathogenicity

Toso (*Faim3*) is an immune-cell-specific surface molecule that negatively regulates *Fas*-mediated apoptosis (Hitoshi et al., 1998) and a member of the module co-varying with regulatory genes (Figure 4B). While this may naively suggest that TOSO would enhance regulatory mechanisms, *Toso*$^{-/-}$ mice are resistant to EAE (Lang et al., 2013). *Toso* could therefore be a negative regulator of the non-pathogenic state.

Supporting this hypothesis, *Toso*$^{-/-}$ cells showed a defect in the production of the pro-inflammatory cytokine IL-17A for both differentiation conditions (Figures 5F and 5G), and memory *Toso*$^{-/-}$ cells stimulated with IL-23 lacked IL-17A production (Figure S7E). In a MOG_{35-55} recall assay, CD3$^+$CD4$^+$ *Toso*$^{-/-}$ T cells showed no IL-17A production (Figure 5H). This supports a role for *Toso* as a promoter of pathogenicity.

Population RNA-seq analysis shows that loss of TOSO results in suppression of the key regulatory genes (e.g., *Il24*, *Il9*, and *Procr*; Table S6), consistent with an IL-10 reduction measured by ELISA (Figure S7G) and a reduced FOXP3$^+$ cell count during Treg differentiation (TGF-β1, Figure S7F). On the other hand, in the pathogenic condition, *Il17a* is downregulated in the absence of TOSO. Enrichment analysis with respect to PC1 of the non-pathogenic condition suggests that *Toso*$^{-/-}$ cells, rather than upregulating regulatory genes, downregulate genes associated with a more pro-inflammatory phenotype (Figure 5E). *Toso* is also bound by *Rorγt* (Ciofani et al., 2012), providing an additional Th17-specific mechanism of action.

MOG_{35-55}-Stimulated *Plzp*$^{-/-}$ Cells Have a Defect in Generating Pathogenic Th17 Cells

The transcription factor *Plzp* (*Rog*, *Zbtb32*) is a known repressor of the Th2 master regulator *Gata3* and regulates cytokine expression (Miaw et al., 2000) in T-helper cells. We hypothesized that *Plzp* regulates pathogenicity in Th17 cells, but we could not undertake an EAE experiment since *Plzp*$^{-/-}$ mice were not available on an EAE-susceptible background.

While in-vitro-differentiated *Plzp*$^{-/-}$ cells produced similar IL-17A levels as WT controls (Figure S7H), a MOG_{35-55} recall assay revealed a defect in IL-17A production, with increasing MOG_{35-55} concentration during restimulation (Figure 5I). When reactivated in the presence of IL-23, which expands in-vivo-generated Th17 cells, *Plzp*$^{-/-}$ cells also produced less IL-17A (Figure S7I). Plzp

Please cite this article in press as: Gaublomme et al., Single-Cell Genomics Unveils Critical Regulators of Th17 Cell Pathogenicity, Cell (2015), http://dx.doi.org/10.1016/j.cell.2015.11.009

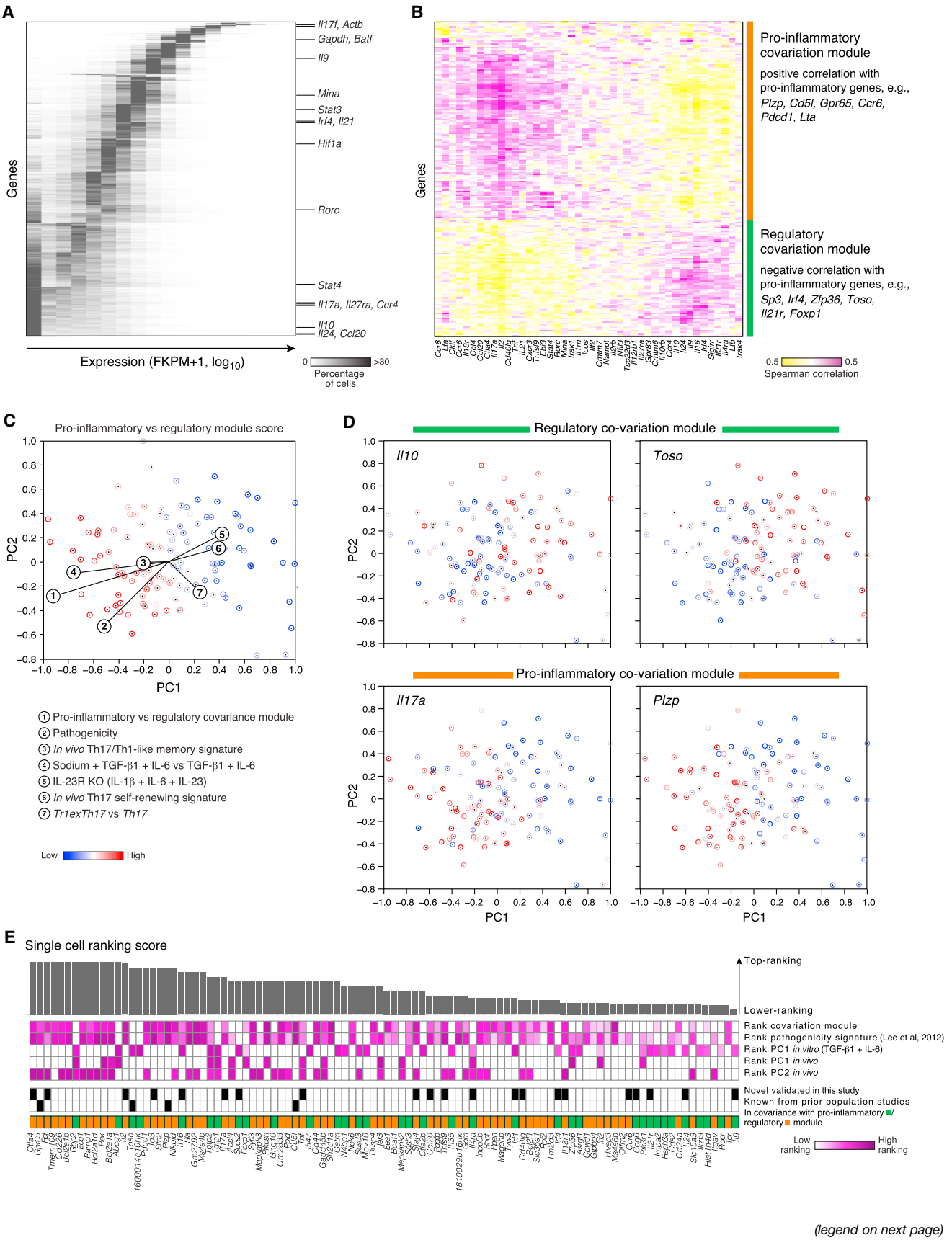

(legend on next page)

appears to influence the expression of a wider range of inflammatory cytokines, as *Plzp*$^{-/-}$ T cells secreted less IL-17A, IL-17F (Figure 5J), IFN-γ, IL-13, and CSF2 (Figure S7J).

Based on RNA-seq profiles at 48 hr of non-pathogenic differentiation of *Plzp*$^{-/-}$ cells, *Irf1*, *Il9*, and other transcripts of the module co-varying with regulatory genes are upregulated (Table S6), whereas transcripts from the module co-varying with pro-inflammatory genes (e.g., *Ccl20*, *Tnf*, *Il17a*) are repressed, and genes characterizing the more pro-inflammatory cells (PC1, Figure 4C) are strongly enriched among the downregulated genes (Figure 5E).

DISCUSSION

Here, we show how variation and co-variation in single-cell profiles can be leveraged to identify key regulatory modules and the factors that may control them to dissect Th17 cell pathogenicity beyond differentiation.

In vivo, we used variation to infer the life cycle of Th17 cells. Processes such as self-renewal, observed in the LN, may provide a pool of cells that are precursors for differentiating Th17 cells to effector/ memory formation in the CNS. The Th1-like phenotype that we observe in the CNS may be the most pathogenic (Bending et al., 2009; Lee et al., 2009; Muranski et al., 2011) and might facilitate memory cell formation, as the entry of Th1 cells into the memory pool is well established (Sallusto et al., 1999). It is unclear whether cells that adopt a Th1 phenotype are stable "double producers" or whether they show plasticity toward a Th1 fate.

We used transcription factor target enrichment analysis in vivo to nominate key regulators of each state. For example, we predict that *Med12*, *Etv6*, and *Zfx* drive the Th17 self-renewing-like subpopulation in the LN. While neither has been linked to Th17 self-renewal, each has been associated with self-renewal and related functions in other cells (Rocha et al., 2010; Hock et al., 2004; Tsuzuki and Seto, 2013; Galan-Caridad et al., 2007). For the pathogenic effector and memory cells observed in the CNS during EAE, we assign a prominent role to known Th17/Th1 transcription factors such as *Hif1a*, *Fosl2*, *Stat4*, and *Rel*.

In vitro, we used strong co-variation, most pronounced under the least pathogenic and most variable conditions to rank candidate genes, such as *Cd5l* and *Gpr65*, based on their association with known regulatory and pro-inflammatory genes. Consistently, a lack of both *Cd5l* and *Gpr65* significantly alters EAE disease progression. Genes similarly associated with pro-inflammatory functions, which we have not yet followed up on, include: *Gem*, *Tmem109*, and *cd226*. Conversely, *Foxp1*, a member of the module co-varying with regulatory genes, was highly expressed in the LN-derived Th17 self-renewing subpopulation and the gut-derived Th17 cells (Figure S3). Foxp1 negatively regulates IL-21, a driver of Th17 generation (Korn et al., 2007), and dampens T cell activation (Wang et al., 2014). Co-variation of a gene with a particular module does not, however, necessarily indicate similar function of this gene with other genes in the module, as we have seen for *Toso*. Another example, *Lag-3*, is upregulated during T-cell activation but suppresses it (Grosso et al., 2007). This is consistent with a model in which regulators with opposite, antagonistic functions are co-regulated.

Whereas population-based expression profiling has identified genes that govern the differentiation states of Th17 cells, single-cell RNA-seq provides new granularity to unveil potent candidates for manipulation of pathogenicity of Th17 cells without affecting nonpathogenic Th17 cells that may be critical for tissue homeostasis and for maintaining barrier functions.

EXPERIMENTAL PROCEDURES

Additional analyses and details are in the Supplemental Experimental Procedures.

Mice, EAE Induction, and Cell Isolation

C57BL/6 WT and *CD4*$^{-/-}$ (2663) mice were obtained from Jackson Laboratory. IL-17A–GFP^{+} mice were obtained from Biocytogen. *Gpr65*$^{-/-}$, *Plzp*$^{-/-}$, and *Toso*$^{-/-}$ mice were provided by Li Yang, Pier Paolo Pandolfi, and John Coligan, respectively. All animals, unless noted otherwise, were housed and maintained in a conventional pathogen-free facility at the Harvard Institute of Medicine in Boston (Supplemental Experimental Procedures). EAE induction and disease analysis, isolation of T cells from EAE mice at the peak of disease, isolation of T cells and in vitro differentiation, isolation of memory cells and recall assays, and isolation of T cells from lamina propria was performed as described in the Supplemental Experimental Procedures.

RNA-Seq

Whole-transcriptome amplification of cell lysates was performed by SMART-seq (Ramsköld et al., 2012) using the Fluidigm C_1 Single-Cell Auto Prep System, followed by Nextera XT DNA Sample Preparation (Illumina), as described in the Supplemental Experimental Procedures. We collected at least two independent biological replicates for each in vivo and in vitro condition and two technical replicates for two in vivo conditions.

RNA-Seq Preprocessing

RNA-seq reads alignment and transcript quantification were performed as described in the Supplemental Experimental Procedures. We used log

Figure 4. Modules of Genes that Co-vary with Pro-inflammatory and Regulatory Genes across Single Cells

(A) Single-cell expression distribution of genes. The heatmap shows for each gene (row) its expression distribution across single cells differentiated under the TGF-β1+IL-6 condition for 48 hr (without further IL-17A-based sorting). Color scale: proportion of cells expressing in each of the 17 expression bins (columns). Genes are sorted from more unimodal (top) to bimodal (bottom).

(B) Modules co-varying with pro-inflammatory and regulatory genes. Heatmap of the Spearman correlation coefficients between the single-cell expression levels of signature genes of pathogenic T cells (Lee et al., 2012) or of other CD4^{+} lineages (columns) and the single-cell expression of any other bimodally expressed gene (rows) in cells differentiated under the TGF-β1+IL-6 condition at 48 hr. Genes are clustered.

(C) The modules co-varying with pro-inflammatory and regulatory genes distinguish key variation. Each cell (TGF-β1+IL-6, 48 hr) is colored by a signature score comparing the two co-variation modules.

(D) Expression of key module genes. Each panel shows the PCA plot of (C) where cells are colored by an expression ranking score of a key gene, denoted on top.

(E) A ranking of the top 100 candidate genes co-varying with pro-inflammatory or regulatory genes (out of 184; Table S5), sorting from high- (left) to lower- (right) ranking scores (bar chart, Supplemental Experimental Procedures).

See also Figures S5 and S6 and Tables S2 and S5 related to Figure 4.

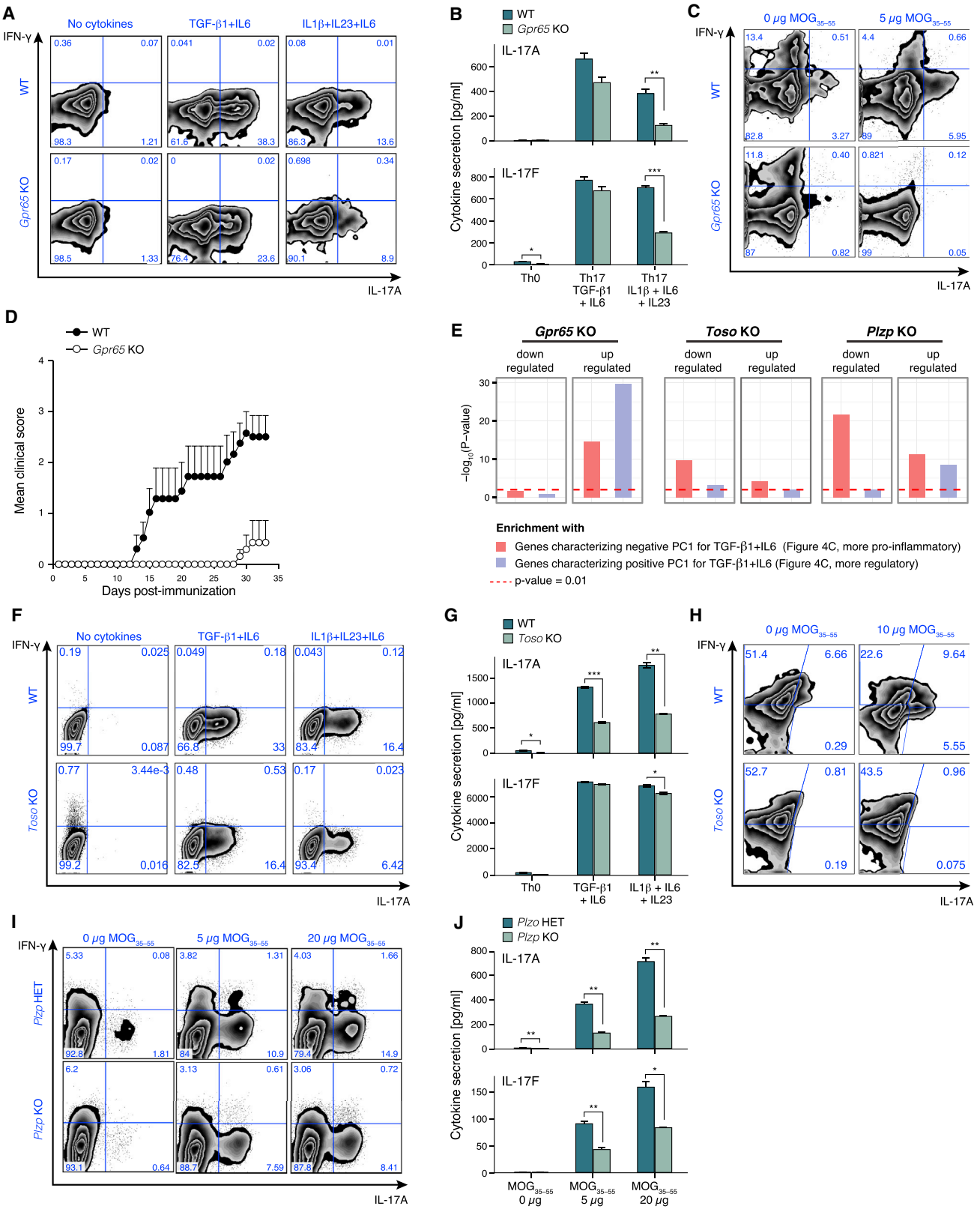

(legend on next page)

transform and quantile normalization to further normalize the expression values (FPKM) within each batch of samples (i.e., all single cells in a given run) and accounted for low (or zero) expression by adding a value of 1 prior to log transform. For each library, we computed quality scores using Fastqc, Picard tools, and in-house scripts, excluding poor libraries from further analysis and further adjusting for the quality scores (Supplemental Experimental Procedures).

Batch Correction

We performed batch correction separately for in vivo and in vitro samples. A filtered gene set consists of the genes that have an expression level exceeding 10 FPKM in at least 20% of the cells of a given sample (Supplemental Experimental Procedures).

Taking into Account False Negatives Using a Weighted Analysis

To account for the effect of each gene's expression and each cell's quality on the probability of false negatives with zero transcript abundance, we construct for each cell a false-negative curve (FNC) representing the false-negative rate as a function of transcript abundance in the bulk population and use this to weight subsequent analyses (Supplemental Experimental Procedures).

Signature Scores and Gene Set Enrichment Analysis

To interpret the functional implications of the variation between cells, we assembled a set of gene signatures that are indicative of various cell states. A typical signature is comprised of a "plus" subset and a "minus" subset. A strong match will have extreme and opposite values for the expression of genes in the two sets (Supplemental Experimental Procedures).

Gene Ranking

We rank genes in the co-variation modules that significantly correlate (Spearman correlation with FDR < 0.05, using the Benjamini-Hochberg scheme) with at least one of the genes in the curated set of bimodally expressed immune response genes (columns of Figure 4B) by five criteria (Supplemental Experimental Procedures): (1) correlation with the first PC in the in-vitro-derived Th17 cells (using TGF-β1+IL6) (2) correlation with the first and (3) second PCs in the in-vivo-derived Th17 cells; (4) correlation with immune-related genes that are specified in the columns of Figure 4B; (5) a similar analysis using a curated pathogenicity signature (genes that are positively or negatively associated with pathogenic Th17 cells based on population-level experiments [Lee et al., 2012]).

ACCESSION NUMBERS

All RNA-seq data are submitted to GEO, with the accession number GEO: GSE74833.

SUPPLEMENTAL INFORMATION

Supplemental Information includes Supplemental Experimental Procedures, seven figures, and seven tables and can be found with this article online at http://dx.doi.org/10.1016/j.cell.2015.11.009.

AUTHOR CONTRIBUTIONS

J.T.G., N.Y., Y.L., A.K.S., V.K.K., H.P. and A.R. conceived the study and designed experiments. A.R. and N.Y. devised analyses, and N.Y. developed computational methods. N.Y., J.T.G., Y.L., and R.S. analyzed the data. J.T.G., Y.L., and R.S.G. conducted the experiments. L.V.Y., P.P.P., and T.M. provided knockout mice. J.T.G, N.Y., V.K.K., H.P., and A.R. wrote the paper with input from all of the authors.

ACKNOWLEDGMENTS

We thank J.E. Coligan for providing *Toso*$^{-/-}$ mice; J. Shuga for scientific discussions; D. Kozoriz, T. Rogers, and M. Tam for assistance with cell sorting; T.J. Diefenbach for assistance with the Imagestream system; C. Wu for help with EAE experiments; O. Rozenblatt-Rosen, E. Shefler, J. Lee, and C. Guiducci for project management; the Broad Genomics Platform for all sequencing work; and L. Gaffney for help with artwork. Work was supported by the Klarman Cell Observatory at the Broad Institute (A.R., H.P., and V.K.K.), an NIH grant P50 HG006193 (A.R. and H.P.), and by the Koch Institute Support (core) grant P30-CA14051 from the National Cancer Institute (A.R.). V.K.K. was supported by NIH grants NS030843, AI039671, NS076410, AI056299, National MS Society, New York, and Crohn's and Colitis Foundation of America. C.W. was supported by a Career Transition Award from the National Multiple Sclerosis Society (TA3059-A-2) and NIH grant 4R00AI110649. R.S. was supported by NIH NSRA grant F32 HD075541. A.R. is an Investigator of the Howard Hughes Medical Institute. During the course of the research, V.K.K. had an ownership interest in Tempero Pharmaceuticals, a company that was working in the area of Treg-Th17 biology and developing treatments for autoimmune diseases in areas related to this research. V.K.K.'s ownership ended in October 2014. V.K.K.'s interests were reviewed and managed by the Brigham and Women's Hospital and Partners HealthCare in accordance with their conflict of interest policies. A.R. is a paid consultant for Driver Group and a member of the SAB of ThermoFisher Scientific and Syros Pharmaceuticals. A.R.'s interests were reviewed and managed by the Broad Institute according to its conflict of interest policies.

Received: March 2, 2015
Revised: August 18, 2015
Accepted: November 3, 2015
Published: November 19, 2015

Figure 5. *Gpr65*, *Toso*, and *Plzp* Are Validated as T Cell Pathogenicity Regulators

(A and B) Reduction in IL17A-producing cells in *Gpr65*$^{-/-}$ T cells differentiated in vitro. (A) Intracellular cytokine staining for IFN-γ and IL-17A of CD4$^+$ WT or *GPR65*$^{-/-}$ cells differentiated for 96 hr. (B) Quantification of secreted IL-17A and Il-17F by cytometric bead assays (CBA) in corresponding samples. *p < 0.05, **p < 0.01, ***p < 0.001. Error bars represent SD; n = 3.

(C) Reduced IL-17A and IFN-γ production by *Gpr65*$^{-/-}$ memory (CD62L$^-$CD44$^+$CD4$^+$) T cells in a recall assay (Supplemental Experimental Procedures).

(D) Loss of GPR65 reduces tissue inflammation and autoimmune disease in vivo. *RAG-1*$^{-/-}$ mice (n = 10 per category) were reconstituted with 2 × 10^6 naive WT or *Gpr65*$^{-/-}$ CD4$^+$ T cells and were induced with EAE 1 week post transfer. Error bars represent SD.

(E) Transcriptional impact of a loss of GPR65, TOSO, and PLZP. Shown is the significance of enrichment ($-\log_{10}$ [p value]; hypergeometric test, y axis) of genes that are dysregulated compared to WT during the TGF-β1+IL-6 differentiation of *Gpr65*$^{-/-}$ (96 hr), *Plzp*$^{-/-}$ (48 hr) and *Toso*$^{-/-}$ (96 hr) cells.

(F and G) Reduction in IL17A-producing cells in *Toso*$^{-/-}$ T cells differentiated in vitro. (F) Intracellular cytokine staining as in (A) but for WT or *Toso*$^{-/-}$ CD4$^+$ T cells activated in vitro for 96 hr. (G) Quantification of secreted IL-17A and IL-17F for WT or *Toso*$^{-/-}$ CD4$^+$ T cells, as in (B). Error bars represent SD; n = 3.

(H) Reduced IL-17A production by *Toso*$^{-/-}$ LN memory T cells in a recall assay as in (C).

(I) Hampered IL-17A production by *Plzp*$^{-/-}$ CD4+ T cells in an in vitro recall assay (Supplemental Experimental Procedures). Intracellular cytokine staining for IFN-γ (y axis) and IL-17A (x axis).

(J) Quantification of secreted IL-17A and IL-17F of a MOG_{35-55} recall assay for littermate controls and *PLZP*$^{-/-}$ mice at 96 hr post ex vivo. All experiments are a representative of at least three independent experiments with at least three experimental replicates per group. Error bars represent SD; n = 3.

See also Figure S7 and Table S6.

REFERENCES

Antebi, Y.E., Reich-Zeliger, S., Hart, Y., Mayo, A., Eizenberg, I., Rimer, J., Putheti, P., Pe'er, D., and Friedman, N. (2013). Mapping differentiation under mixed culture conditions reveals a tunable continuum of T cell fates. PLoS Biol. *11*, e1001616.

Aust, G., Kamprad, M., Lamesch, P., and Schmucking, E. (2005). CXCR6 within T-helper (Th) and T-cytotoxic (Tc) type 1 lymphocytes in Graves' disease (GD). Eur. J. Endocrinol. *152*, 635–643.

Bending, D., De la Peña, H., Veldhoen, M., Phillips, J.M., Uyttenhove, C., Stockinger, B., and Cooke, A. (2009). Highly purified Th17 cells from BDC2.5NOD mice convert into Th1-like cells in NOD/SCID recipient mice. J. Clin. Invest. *119*, 565–572.

Blaschitz, C., and Raffatellu, M. (2010). Th17 cytokines and the gut mucosal barrier. J. Clin. Immunol. *30*, 196–203.

Ciofani, M., Madar, A., Galan, C., Sellars, M., Mace, K., Pauli, F., Agarwal, A., Huang, W., Parkurst, C.N., Muratet, M., et al. (2012). A validated regulatory network for Th17 cell specification. Cell *151*, 289–303.

Cortes, A., Hadler, J., Pointon, J.P., Robinson, P.C., Karaderi, T., Leo, P., Cremin, K., Pryce, K., Harris, J., Lee, S., et al.; International Genetics of Ankylosing Spondylitis Consortium (IGAS); Australo-Anglo-American Spondyloarthritis Consortium (TASC); Groupe Française d'Etude Génétique des Spondylarthrites (GFEGS); Nord-Trøndelag Health Study (HUNT); Spondyloarthritis Research Consortium of Canada (SPARCC); Wellcome Trust Case Control Consortium 2 (WTCCC2) (2013). Identification of multiple risk variants for ankylosing spondylitis through high-density genotyping of immune-related loci. Nat. Genet. *45*, 730–738.

Crawford, A., Angelosanto, J.M., Kao, C., Doering, T.A., Odorizzi, P.M., Barnett, B.E., and Wherry, E.J. (2014). Molecular and transcriptional basis of $CD4^+$ T cell dysfunction during chronic infection. Immunity *40*, 289–302.

De Rosa, S.C., Herzenberg, L.A., Herzenberg, L.A., and Roederer, M. (2001). 11-color, 13-parameter flow cytometry: identification of human naive T cells by phenotype, function, and T-cell receptor diversity. Nat. Med. *7*, 245–248.

Deng, Q., Ramsköld, D., Reinius, B., and Sandberg, R. (2014). Single-cell RNA-seq reveals dynamic, random monoallelic gene expression in mammalian cells. Science *343*, 193–196.

Dolfi, D.V., Boesteanu, A.C., Petrovas, C., Xia, D., Butz, E.A., and Katsikis, P.D. (2008). Late signals from CD27 prevent Fas-dependent apoptosis of primary CD8+ T cells. J. Immunol. *180*, 2912–2921.

Esplugues, E., Huber, S., Gagliani, N., Hauser, A.E., Town, T., Wan, Y.Y., O'Connor, W., Jr., Rongvaux, A., Van Rooijen, N., Haberman, A.M., et al. (2011). Control of TH17 cells occurs in the small intestine. Nature *475*, 514–518.

Fischer, M.T., Wimmer, I., Hoftberger, R., Gerlach, S., Haider, L., Zrzavy, T., Hametner, S., Mahad, D., Binder, C.J., Krumbholz, M., et al. (2013). Disease-specific molecular events in cortical multiple sclerosis lesions. Brain *136*, 1799–1815.

Franke, A., McGovern, D.P., Barrett, J.C., Wang, K., Radford-Smith, G.L., Ahmad, T., Lees, C.W., Balschun, T., Lee, J., Roberts, R., et al. (2010). Genome-wide meta-analysis increases to 71 the number of confirmed Crohn's disease susceptibility loci. Nat. Genet. *42*, 1118–1125.

Gagliani, N., Vesely, M.C., Iseppon, A., Brockmann, L., Xu, H., Palm, N.W., de Zoete, M.R., Licona-Limón, P., Paiva, R.S., Ching, T., et al. (2015). Th17 cells transdifferentiate into regulatory T cells during resolution of inflammation. Nature *523*, 221–225.

Galan-Caridad, J.M., Harel, S., Arenzana, T.L., Hou, Z.E., Doetsch, F.K., Mirny, L.A., and Reizis, B. (2007). Zfx controls the self-renewal of embryonic and hematopoietic stem cells. Cell *129*, 345–357.

Ghoreschi, K., Laurence, A., Yang, X.P., Tato, C.M., McGeachy, M.J., Konkel, J.E., Ramos, H.L., Wei, L., Davidson, T.S., Bouladoux, N., et al. (2010). Generation of pathogenic T(H)17 cells in the absence of TGF-β signalling. Nature *467*, 967–971.

Gilmore, T.D., and Gerondakis, S. (2011). The c-Rel Transcription Factor in Development and Disease. Genes Cancer *2*, 695–711.

Grosso, J.F., Kelleher, C.C., Harris, T.J., Maris, C.H., Hipkiss, E.L., De Marzo, A., Anders, R., Netto, G., Getnet, D., Bruno, T.C., et al. (2007). LAG-3 regulates CD8+ T cell accumulation and effector function in murine self- and tumor-tolerance systems. J. Clin. Invest. *117*, 3383–3392.

Hendriks, J., Gravestein, L.A., Tesselaar, K., van Lier, R.A., Schumacher, T.N., and Borst, J. (2000). CD27 is required for generation and long-term maintenance of T cell immunity. Nat. Immunol. *1*, 433–440.

Hernández-Santos, N., and Gaffen, S.L. (2012). Th17 cells in immunity to Candida albicans. Cell Host Microbe *11*, 425–435.

Hilliard, B.A., Mason, N., Xu, L., Sun, J., Lamhamedi-Cherradi, S.E., Liou, H.C., Hunter, C., and Chen, Y.H. (2002). Critical roles of c-Rel in autoimmune inflammation and helper T cell differentiation. J. Clin. Invest. *110*, 843–850.

Hitoshi, Y., Lorens, J., Kitada, S.I., Fisher, J., LaBarge, M., Ring, H.Z., Francke, U., Reed, J.C., Kinoshita, S., and Nolan, G.P. (1998). Toso, a cell surface, specific regulator of Fas-induced apoptosis in T cells. Immunity *8*, 461–471.

Hock, H., Meade, E., Medeiros, S., Schindler, J.W., Valk, P.J., Fujiwara, Y., and Orkin, S.H. (2004). Tel/Etv6 is an essential and selective regulator of adult hematopoietic stem cell survival. Genes Dev. *18*, 2336–2341.

Holzer, U., Reinhardt, K., Lang, P., Handgretinger, R., and Fischer, N. (2013). Influence of a mutation in IFN-γ receptor 2 (IFNGR2) in human cells on the generation of Th17 cells in memory T cells. Hum. Immunol. *74*, 693–700.

Jostins, L., Ripke, S., Weersma, R.K., Duerr, R.H., McGovern, D.P., Hui, K.Y., Lee, J.C., Schumm, L.P., Sharma, Y., Anderson, C.A., et al.; International IBD Genetics Consortium (IIBDGC) (2012). Host-microbe interactions have shaped the genetic architecture of inflammatory bowel disease. Nature *491*, 119–124.

Komatsu, N., Okamoto, K., Sawa, S., Nakashima, T., Oh-hora, M., Kodama, T., Tanaka, S., Bluestone, J.A., and Takayanagi, H. (2014). Pathogenic conversion of Foxp3+ T cells into TH17 cells in autoimmune arthritis. Nat. Med. *20*, 62–68.

Korn, T., Bettelli, E., Gao, W., Awasthi, A., Jäger, A., Strom, T.B., Oukka, M., and Kuchroo, V.K. (2007). IL-21 initiates an alternative pathway to induce proinflammatory T(H)17 cells. Nature *448*, 484–487.

Korn, T., Bettelli, E., Oukka, M., and Kuchroo, V.K. (2009). IL-17 and Th17 Cells. Annu. Rev. Immunol. *27*, 485–517.

Kryczek, I., Zhao, E., Liu, Y., Wang, Y., Vatan, L., Szeliga, W., Moyer, J., Klimczak, A., Lange, A., and Zou, W. (2011). Human TH17 cells are long-lived effector memory cells. Sci. Transl. Med. *3*, 104ra100.

Lang, K.S., Lang, P.A., Meryk, A., Pandyra, A.A., Boucher, L.M., Pozdeev, V.I., Tusche, M.W., Göthert, J.R., Haight, J., Wakeham, A., et al. (2013). Involvement of Toso in activation of monocytes, macrophages, and granulocytes. Proc. Natl. Acad. Sci. USA *110*, 2593–2598.

Lee, Y.K., Turner, H., Maynard, C.L., Oliver, J.R., Chen, D., Elson, C.O., and Weaver, C.T. (2009). Late developmental plasticity in the T helper 17 lineage. Immunity *30*, 92–107.

Lee, Y., Awasthi, A., Yosef, N., Quintana, F.J., Xiao, S., Peters, A., Wu, C., Kleinewietfeld, M., Kunder, S., Hafler, D.A., et al. (2012). Induction and molecular signature of pathogenic TH17 cells. Nat. Immunol. *13*, 991–999.

Liberzon, A., Subramanian, A., Pinchback, R., Thorvaldsdóttir, H., Tamayo, P., and Mesirov, J.P. (2011). Molecular signatures database (MSigDB) 3.0. Bioinformatics *27*, 1739–1740.

Mahad, D.J., and Ransohoff, R.M. (2003). The role of MCP-1 (CCL2) and CCR2 in multiple sclerosis and experimental autoimmune encephalomyelitis (EAE). Semin. Immunol. *15*, 23–32.

Miaw, S.C., Choi, A., Yu, E., Kishikawa, H., and Ho, I.C. (2000). ROG, repressor of GATA, regulates the expression of cytokine genes. Immunity *12*, 323–333.

Mo, C., Chearwae, W., O'Malley, J.T., Adams, S.M., Kanakasabai, S., Walline, C.C., Stritesky, G.L., Good, S.R., Perumal, N.B., Kaplan, M.H., and Bright, J.J. (2008). Stat4 isoforms differentially regulate inflammation and demyelination in experimental allergic encephalomyelitis. J. Immunol. *181*, 5681–5690.

Muranski, P., Borman, Z.A., Kerkar, S.P., Klebanoff, C.A., Ji, Y., Sanchez-Perez, L., Sukumar, M., Reger, R.N., Yu, Z., Kern, S.J., et al. (2011). Th17 cells

are long lived and retain a stem cell-like molecular signature. Immunity *35*, 972–985.

Nakae, S., Iwakura, Y., Suto, H., and Galli, S.J. (2007). Phenotypic differences between Th1 and Th17 cells and negative regulation of Th1 cell differentiation by IL-17. J. Leukoc. Biol. *81*, 1258–1268.

O'Connor, W., Jr., Kamanaka, M., Booth, C.J., Town, T., Nakae, S., Iwakura, Y., Kolls, J.K., and Flavell, R.A. (2009). A protective function for interleukin 17A in T cell-mediated intestinal inflammation. Nat. Immunol. *10*, 603–609.

Okada, Y., Wu, D., Trynka, G., Raj, T., Terao, C., Ikari, K., Kochi, Y., Ohmura, K., Suzuki, A., Yoshida, S., et al.; RACI consortium; GARNET consortium (2014). Genetics of rheumatoid arthritis contributes to biology and drug discovery. Nature *506*, 376–381.

Perfetto, S.P., Chattopadhyay, P.K., and Roederer, M. (2004). Seventeen-colour flow cytometry: unravelling the immune system. Nat. Rev. Immunol. *4*, 648–655.

Ramsköld, D., Luo, S., Wang, Y.-C., Li, R., Deng, Q., Faridani, O.R., Daniels, G.A., Khrebtukova, I., Loring, J.F., Laurent, L.C., et al. (2012). Full-length mRNA-Seq from single-cell levels of RNA and individual circulating tumor cells. Nat. Biotechnol. *30*, 777–782.

Reya, T., Duncan, A.W., Ailles, L., Domen, J., Scherer, D.C., Willert, K., Hintz, L., Nusse, R., and Weissman, I.L. (2003). A role for Wnt signalling in self-renewal of haematopoietic stem cells. Nature *423*, 409–414.

Rocha, P.P., Scholze, M., Bleiss, W., and Schrewe, H. (2010). Med12 is essential for early mouse development and for canonical Wnt and Wnt/PCP signaling. Development *137*, 2723–2731.

Sallusto, F., Lenig, D., Förster, R., Lipp, M., and Lanzavecchia, A. (1999). Two subsets of memory T lymphocytes with distinct homing potentials and effector functions. Nature *401*, 708–712.

Sawcer, S., Hellenthal, G., Pirinen, M., Spencer, C.C., Patsopoulos, N.A., Moutsianas, L., Dilthey, A., Su, Z., Freeman, C., Hunt, S.E., et al.; International Multiple Sclerosis Genetics Consortium; Wellcome Trust Case Control Consortium 2 (2011). Genetic risk and a primary role for cell-mediated immune mechanisms in multiple sclerosis. Nature *476*, 214–219.

Shalek, A.K., Satija, R., Adiconis, X., Gertner, R.S., Gaublomme, J.T., Raychowdhury, R., Schwartz, S., Yosef, N., Malboeuf, C., Lu, D., et al. (2013). Single-cell transcriptomics reveals bimodality in expression and splicing in immune cells. Nature *498*, 236–240.

Shalek, A.K., Satija, R., Shuga, J., Trombetta, J.J., Gennert, D., Lu, D., Chen, P., Gertner, R.S., Gaublomme, J.T., Yosef, N., et al. (2014). Single-cell RNA-seq reveals dynamic paracrine control of cellular variation. Nature *510*, 363–369.

Trapnell, C., Cacchiarelli, D., Grimsby, J., Pokharel, P., Li, S., Morse, M., Lennon, N.J., Livak, K.J., Mikkelsen, T.S., and Rinn, J.L. (2014). The dynamics and regulators of cell fate decisions are revealed by pseudotemporal ordering of single cells. Nat. Biotechnol. *32*, 381–386.

Tsuzuki, S., and Seto, M. (2013). TEL (ETV6)-AML1 (RUNX1) initiates self-renewing fetal pro-B cells in association with a transcriptional program shared with embryonic stem cells in mice. Stem Cells *31*, 236–247.

Wang, H., Geng, J., Wen, X., Bi, E., Kossenkov, A.V., Wolf, A.I., Tas, J., Choi, Y.S., Takata, H., Day, T.J., et al. (2014). The transcription factor Foxp1 is a critical negative regulator of the differentiation of follicular helper T cells. Nat. Immunol. *15*, 667–675.

Wang, C., Yosef, N., Gaublomme, J., Wu, C., Lee, Y., Clish, C.B., Kaminski, J., Xiao, S., Zu Horste, G.M., Pawlak, M., et al. (2015). CD5L/AIM regulates lipid biosynthesis and restrains Th17 cell pathogenicity. Cell *163*. Published online November 19, 2015. http://dx.doi.org/10.1016/j.cell.2015.10.068.

Wherry, E.J., Ha, S.J., Kaech, S.M., Haining, W.N., Sarkar, S., Kalia, V., Subramaniam, S., Blattman, J.N., Barber, D.L., and Ahmed, R. (2007). Molecular signature of CD8+ T cell exhaustion during chronic viral infection. Immunity *27*, 670–684.

Wu, C., Yosef, N., Thalhamer, T., Zhu, C., Xiao, S., Kishi, Y., Regev, A., and Kuchroo, V.K. (2013). Induction of pathogenic TH17 cells by inducible salt-sensing kinase SGK1. Nature *496*, 513–517.

Yosef, N., Shalek, A.K., Gaublomme, J.T., Jin, H., Lee, Y., Awasthi, A., Wu, C., Karwacz, K., Xiao, S., Jorgolli, M., et al. (2013). Dynamic regulatory network controlling TH17 cell differentiation. Nature *496*, 461–468.